IONIC TRANSPORT IN A CONTINUOUS DONNAN DIALYZER WITH TWO PARALLEL-PLATE CHANNELS

KAZUHISA SATO, TETSUYA SAKAIRI, TOSHIKUNI YONEMOTO AND TEIRIKI TADAKI

Department of Biochemistry and Engineering, Tohoku University, Sendai 980

Key Words: Membrane Separation, Ion Exchange Membrane, Mass Transfer, Numerical Simulation, Donnan Dialysis

Ionic transport in a continuous Donnan dialyzer with two parallel-plate channels was studied for a bi-ionic exchange system. A theoretical model of the system was formulated on the basis of diffusion equations in terms of diffusion, migration and convection of each ion. Theoretical solutions were obtained by numerical calculations using a finite-difference technique. Simultaneously, continuous Donnan dialytic experiments with a cation-exchange membrane were conducted for the K^+–H^+ and Ca^{2+}–H^+ exchange systems. The validity of the model and the numerical calculations was confirmed by comparison with experimental results for mean dialytic rates. The numerical calculation also provided distributions of ionic concentrations in both the channels and the membrane, and the electric potential in the channels. An effectiveness factor was introduced to investigate the proportion of the mass transfer resistance in the membrane phase or the liquid phase to its overall value. The influence of Reynolds number, channel height and valence of counter-ion on the mean dialytic rates and on the effectiveness factor was also discussed.

Introduction

Donnan dialysis is expected to be applied in many ionic separation processes from an energy-saving point of view.

In our previous paper,[7] we analyzed an ionic transport process in a continuous Donnan dialyzer with a parallel-plate channel and an agitated tank and quantitatively examined the effects of Reynolds number and parallel-plate channel height on the dialytic rate.

Most dialyzers in industrial separation processes, however, have parallel-plate channels with small gaps on both sides of the membrane. This is because a larger ratio of effective membrane area to dialyzer volume is desired. The theoretical analysis for such a dialyzer may be more complicated than the previous one,[7] since ionic transport processes in two parallel-plate channels and the ion-exchange membrane must be considered simultaneously.

In this paper, we deal with an ionic transport process in a dialyzer with two parallel-plate channels, in which bi-ionic exchange occurs between the solutions flowing in the two channels. A theoretical model of the system is formulated on the basis of a mass transfer equation in terms of diffusion, migration and convection. The model equations are solved numerically. The influence of Reynolds number, channel height and valence of counter-ion on the dialytic rate is discussed, with a comparison of the numerical results and experimental ones for K^+–H^+ and Ca^{2+}–H^+ exchange systems.

1. Theory

Consider a continuous ion-exchange system such as that shown in **Fig. 1.** A cation-exchange membrane separates the parallel-plate channels from each other. KCl (or $CaCl_2$) aqueous solution in channel *A* and HCl aqueous solution in channel *B* flow cocurrently. The ion exchange of K^+ (or Ca^{2+}) and H^+ occurs across the membrane. It is assumed that fully developed laminar flows are attained in both channels.

First, consider the membrane-phase mass trans-

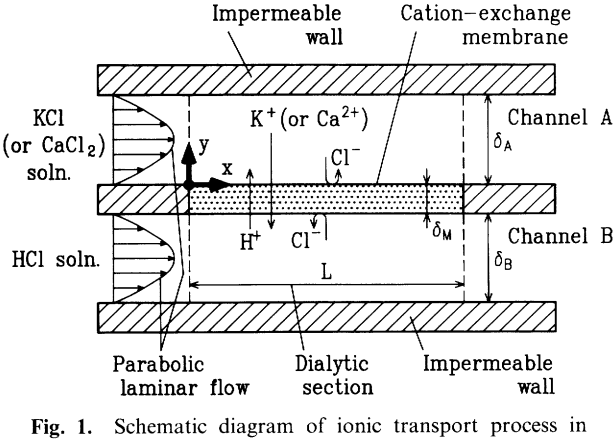

Fig. 1. Schematic diagram of ionic transport process in Donnan dialyzer with two parallel-plate channels

* Received March 6, 1991. Correspondence concerning this article should be addressed to T. Tadaki.

port. If counter-ions K^+ (or Ca^2) and H^+ move only in the y direction and no co-ion Cl^- exists in the membrane, the mass flux of each ion in the membrane, $\bar{N}_i$, is represented on the basis of the Nernst–Planck equation, as follows[6,7]:

$$\bar{N}_1 = -\frac{1}{\delta_M}\cdot\frac{\bar{D}_1\bar{D}_2}{\bar{D}_1 n_1 - \bar{D}_2 n_2}\left[(n_1-n_2)(\bar{C}_{1,A}-\bar{C}_{1,B}) - \frac{n_2 n_F Q(\bar{D}_1-\bar{D}_2)}{\bar{D}_1 n_1 - \bar{D}_2 n_2} \times \ln\left\{\frac{n_1(\bar{D}_1 n_1 - \bar{D}_2 n_2)\bar{C}_{1,A} - \bar{D}_2 n_2 Q n_F}{n_1(\bar{D}_1 n_1 - \bar{D}_2 n_2)\bar{C}_{1,B} - \bar{D}_2 n_2 Q n_F}\right\}\right] \quad (1)$$

$$\bar{N}_2 = -\frac{n_1}{n_2}\bar{N}_1 \quad (2)$$

$$\bar{N}_3 = 0 \quad (3)$$

where subscript $i=1$ refers to K^+ (or Ca^{2+}), and 2 and 3 refer to H^+ and Cl^- respectively.

Next, consider the solution-phase mass transport in channels in a manner similar to that in the previous analysis.[7] When we take account of the ionic transport owing to convection in the x direction and owing to diffusion and migration in the y direction, the diffusion equation of each ion becomes

$$u_h\frac{\partial C_{h,i}}{\partial x} - D_i\frac{\partial}{\partial y}\left\{\frac{\partial C_{h,i}}{\partial y} + \frac{n_i C_{h,i} F}{RT}\cdot\frac{\partial \phi}{\partial y}\right\} = 0 \quad (4)$$
$$(h=A,\ B,\quad i=1,\ 2,\ 3)$$

where subscript h refers to each channel, and the term in brackets multiplied by $-D_i$ represents the ionic flux in the direction of the y axis, N_i. Eliminating the term of the electric potential gradient from Eq. (4) by using the electroneutrality condition and introducing dimensionless numbers gives[7]

$$U_h\frac{\partial Z_{h,i}}{(\delta_A/\delta_h)\partial X} - S_{h,i}\frac{\partial^2 Z_{h,i}}{\partial {Y_h}^2} + S_{h,i}n_i\frac{\partial}{\partial Y_h}\left\{Z_{h,i}\frac{\sum_{\xi}^{3} S_{h,\xi}n_\xi(\partial Z_{h,\xi}/\partial Y_h)}{\sum_{\xi}^{3} S_{h,\xi}{n_\xi}^2 Z_{h,\xi}}\right\} = 0 \quad (5)$$

where dimensionless velocity, U, is given as

$$U_h = Y_h - {Y_h}^2 \quad (6)$$

The initial conditions at the inlet of each channel are

$$X=0,\quad Z_{h,i}=Z_{h,i}|_{\text{in}} \quad (h=A,\ B\quad i=1,\ 2,\ 3) \quad (7)$$

At the membrane-solution interface on each channel side, $Y_h=0$, the dimensionless flux of the membrane phase is equal to that of the liquid phase, and the equilibrium relation holds so that

$$Y_h=0;\quad \mathcal{N}_{h,i} = \bar{N}_i/6\bar{u}_A Q \quad \text{for} \quad h=A\ (i=1,2)$$
$$-\bar{N}_i/6\bar{u}_B Q \quad \text{for} \quad h=B\ (i=1,2)$$
$$\mathcal{N}_{h,3}=0 \quad (h=A,\ B) \quad (8)$$

$${K_2}^1 = \frac{\bar{C}_1^{|n_2|}\cdot C_{h,2}^{|n_1|}}{C_{h,1}^{|n_2|}\cdot\bar{C}_2^{|n_1|}} = \frac{\bar{C}_1^{|n_2|}\cdot Z_{h,2}^{|n_1|}}{Z_{h,1}^{|n_2|}\cdot\bar{C}_2^{|n_1|}} Q^{|n_1|-|n_2|} \quad (h=A,\ B) \quad (9)$$

where ${K_2}^1$ is the selectivity coefficient.[1)]

The boundary conditions at the impermeable walls are

$$Y_h=1;\quad \mathcal{N}_{h,i}=0 \quad (h=A,\ B\quad i=1,\ 2,\ 3) \quad (10)$$

Equation (5) was finite-differentiated and then solved numerically by the Newton–Raphson iterative technique under restrictions (6) to (10) in a manner similar to that in a previous paper.[7]

The concentration of the outlet of each channel was obtained by calculating the mixing cap average concentration[7] as follows:

$$Z_{h,i}|_{\text{out}} = \frac{\int_0^1 Z_{h,i}|_{X=L/\delta_A} U_h\cdot dY_h}{\int_0^1 U_h\cdot dY_h} \quad (11)$$

Physical properties used in the numerical calculations are listed in **Table 1**. For the Ca^{2+}–H^+ exchange system, the selectivity coefficient and the ionic diffusion coefficients in the membrane were measured in the same way as in a previous work.[6] The ionic diffusion coefficients in the solution phase were estimated.[3,5] The others are the same as in the previous paper.[7]

2. Experimental

Figure 2 shows the Donnan dialyzer used. Two end-plates were made of acrylic resin. The cation-exchange membrane was Neosepta CM-1 of Tokuyama Soda Co., Ltd. The membrane was fastened between the end-plates with silicone rubber gaskets. Each channel was 1.8×10^{-3} m in height (δ_A or δ_B) and 3.00×10^{-2} m in width (W). The surface of the membrane was coated with polyvinyl chloride film except for a dialytic section 2.00×10^{-1} m in length, L, in the middle of the membrane. The effective area of permeation, A_{eff}, therefore, was 6.00×10^{-3} m^2.

Aqueous solutions of 100 mol·m^{-3} KCl (or 50 mol·m^{-3} $CaCl_2$) and 100 mol·m^{-3} HCl were fed into channels A and B at the same Reynolds number of 2–100, respectively.

The outlet concentrations at steady state were determined by an ion chromatograph IC-200 (Yokogawa Electric Co., Ltd.) for K^+ and an ICP emission spectrometer SPS-1200 (Seiko Instruments

Table 1. Physical properties and other parameters used in numerical calculation

for solution phase:		
Diffusion coefficients,	D_i	
	$i=K^+$	1.95×10^{-9} m^2/s
	Ca^{2+}	7.92×10^{-10} m^2/s
	H^+	9.31×10^{-9} m^2/s
	Cl^-	2.03×10^{-9} m^2/s
Kinematic viscosity, v		8.97×10^{-7} m^2/s
for cation-exchange membrane:		
Thickness, δ_M		1.44×10^{-4} m
Ion exchange capacity, Q		2.10×10^{3} mol/m^3
Valence of fixed ion, n_F		-1
Diffusion coefficients, $\bar{D}_i$		
K^+–H^+ system:	$i=K^+$	1.35×10^{-10} m^2/s
	H^+	4.80×10^{-10} m^2/s
Ca^{2+}–H^+ system:	$i=Ca^{2+}$	7.65×10^{-12} m^2/s
	H^+	3.61×10^{-10} m^2/s
Selectivity coefficients*		
K^+–H^+ system:	$\ln K_H^K$	$=1.11-1.06X_K$
Ca^{2+}–H^+ system:	$\ln K_H^{Ca}$	$=1.98-2.59X_{Ca}+8.94X_{Ca}^2-6.35X_{Ca}^3$
Dimensions of parallel-plate channel:		
Length of dialytic section, L		2.00×10^{-1} m
Width of channel, W		3.00×10^{-2} m

* $K_H^K=\dfrac{\bar{C}_K\cdot C_H}{C_K\cdot\bar{C}_H}$, $X_K=\dfrac{C_K}{C_K+C_H}$

$K_H^{Ca}=\dfrac{\bar{C}_{Ca}\cdot C_H^2}{C_{Ca}\cdot\bar{C}_H^2}$, $X_{Ca}=\dfrac{2C_{Ca}}{2C_{Ca}+C_H}$

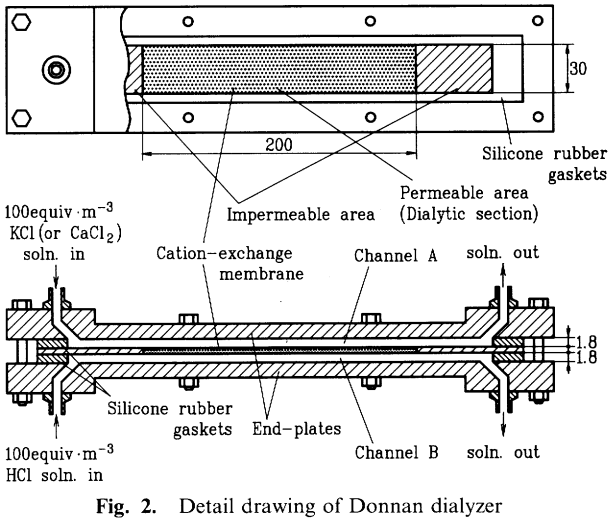

Fig. 2. Detail drawing of Donnan dialyzer

Inc.) for Ca^{2+}.

Experiments were conducted at 298 ± 0.5 K by using a temperature-controlled water bath.

3. Results and Discussion

The mean dialytic rate, $\mathscr{M}_i$,

$$\mathscr{M}_i=\frac{(C_{B,i}|_{out}-C_{B,i}|_{in})\cdot n_i\cdot\bar{u}_B\cdot\delta_B\cdot W}{A_{eff}} \qquad (12)$$

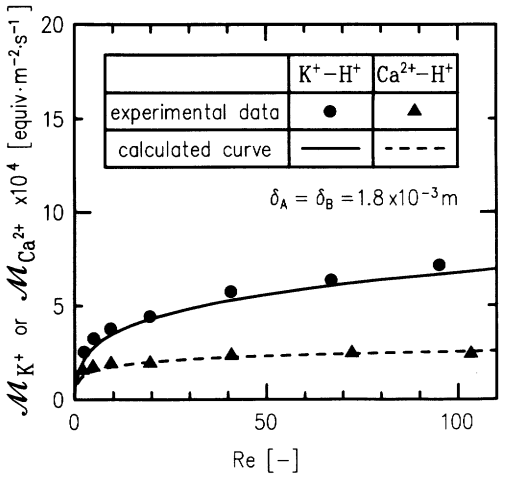

Fig. 3. Theoretical and experimental mean dialytic rates ($Re_A=Re_B$)

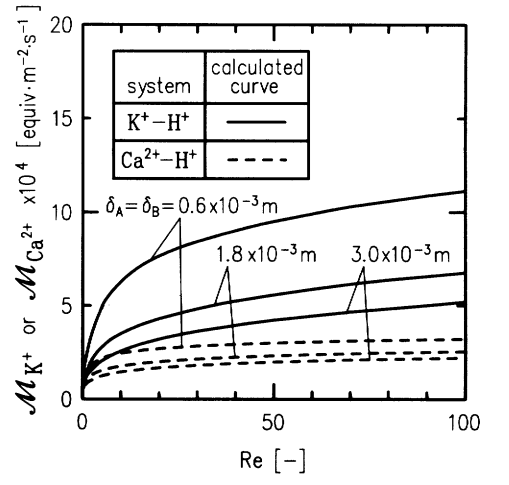

Fig. 4. Effect of channel height on mean dialytic rate ($Re_A=Re_B$)

is first introduced to compare the theoretical results with the experimental ones as in the previous work.[7] **Figure 3** shows the theoretical and experimental mean dialytic rates for $\delta_A=\delta_B=1.8\times10^{-3}$ m. It can be seen from the figure that $\mathscr{M}_i$ increases with Re for both the K^+–H^+ and Ca^{2+}–H^+ exchange systems. In the region of $Re>20$, however, $\mathscr{M}_i$ for the Ca^{2+}–H^+ system increases slightly, although $\mathscr{M}_i$ for the K^+–H^+ system still shows a tendency to rise. $\mathscr{M}_i$ for the K^+–H^+ system is larger than that for the Ca^{2+}–H^+ system. As will be discussed later, this change in $\mathscr{M}_i$ is associated with the relative magnitude of the mass transfer resistance in the membrane phase. For both the K^+–H^+ and Ca^{2+}–H^+ systems, the experimental data agree with the calculated lines at any Re. The model formulation and the calculation procedure, therefore, were considered to be valid.

Figure 4 shows the influence of channel height on mean dialytic rates. It can be seen for both exchange systems that $\mathscr{M}_i$ decreases with channel height. This

is the same as in the case of the previous paper,[7] where the dialyzer had one parallel-plate channel.

Distributions of the ionic concentrations and the electric potential in the direction of the y axis are shown in **Fig. 5** for the K^+–H^+ system and in **Fig. 6** for the Ca^{2+}–H^+ system. For both exchange systems, concentration gradients increase with Re in both the channels and the membrane. These phenomena correspond to the increase in $\mathscr{M}_i$ with Re in Fig. 3. While approaching the membrane, the dimensionless electric potential, Φ, decreases in channel A, and, in contrast, increases in channel B. The potential gradients form for the following reason. For the K^+–H^+ system, K^+ and H^+ have different mobilities and diffuse in the counterdirection along the y axis in each channel. The potential increases in the direction in which H^+, which has larger mobility, diffuses. For the Ca^{2+}–H^+ system, a similar potential gradient also forms because the mobility of H^+ is larger than that of Ca^{2+}. For both exchange systems, the chloride ion migrates away from the membrane in channel A and migrates close to the membrane in channel B due to the potential gradient.

In the membrane, K^+ accounts for 60 to 70 percent of the counter-ions in the K^+–H^+ system, but Ca^{2+} accounts for more than 90 percent of them in the Ca^{2+}–H^+ system. Particularly in the latter system, the Ca^{2+} concentration in the membrane at the membrane-solution interface on the channel A side is close to the ion-exchange capacity even at lower Re. The increase in concentration, therefore, is very small when Re rises from 5 to 100. In this way, the selectivity of Ca^{2+} to H^+ for uptake into the membrane is higher than that of K^+ to H^+. The Donnan potential,[2] which arises at the interface and causes different effects on ions of different valence, may be responsible for the fact mentioned above.

Figure 7 shows contours of ionic concentrations in both channels. Concentration boundary layers are formed at the membrane-liquid interfaces from the starting point of the dialytic section. Figure 7(c) shows nonuniform concentration distributions of the co-ion, Cl^-, as discussed above.

An effectiveness factor[7] η is introduced to investigate the proportion of the mass transfer resistance in the membrane phase to the overall mass transfer resistance:

$$\eta = \frac{(\mathscr{M}_i \text{ calculated considering liquid-phase mass transfer resistance in both channels})}{(\mathscr{M}_i \text{ calculated ignoring liquid-phase mass transfer resistance in both channels})} \quad (13)$$

The denominator of Eq. (13) is the mean dialytic rate calculated by assuming the concentration in both channels to be constant in the direction of the y axis.

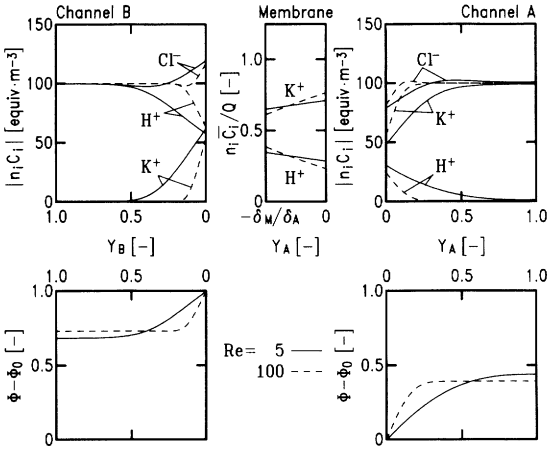

Fig. 5. Theoretical distributions of ionic concentration and electric potential along the y axis for K^+–H^+ system ($X=55.6$, $\delta_A=\delta_B=1.8\times10^{-3}$ m, $Re_A=Re_B$)

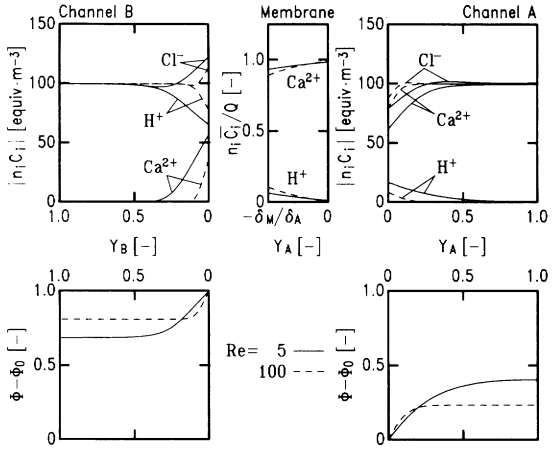

Fig. 6. Theoretical distributions of ionic concentration and electric potential along the y axis for Ca^{2+}–H^+ system ($X=55.6$, $\delta_A=\delta_B=1.8\times10^{-3}$ m, $Re_A=Re_B$)

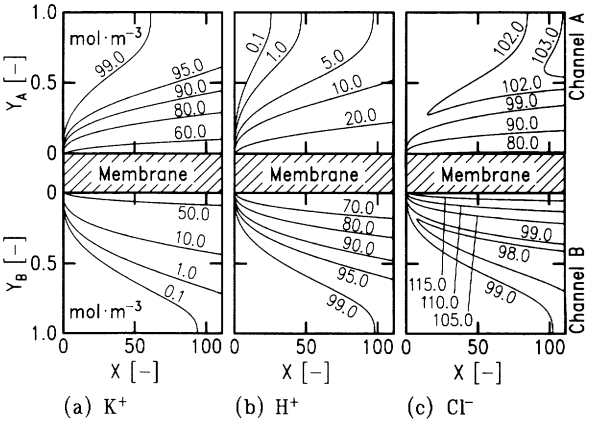

Fig. 7. Theoretical contours of ionic concentrations in parallel-plate channels for K^+–H^+ system ($\delta_A=\delta_B=1.8\times10^{-3}$ m, $Re_A=Re_B=5.0$)

Figure 8 shows the calculated η values. For both exchange systems, as δ_A and δ_B become smaller the dialysis becomes more effective as in the previous

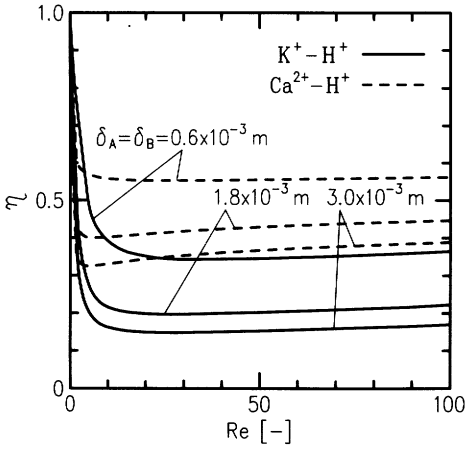

Fig. 8. Theoretical effectiveness factor ($Re_A = Re_B$)

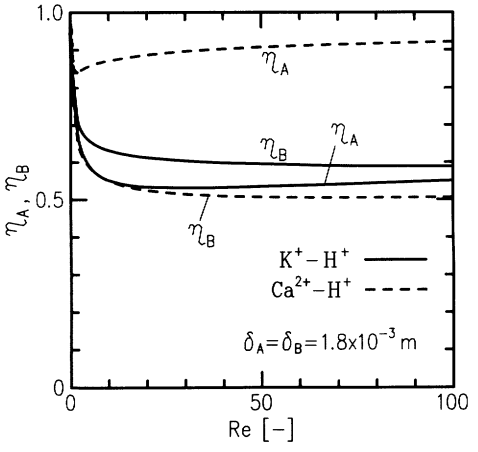

Fig. 9. Theoretical effectiveness factor for each channel ($Re_A = Re_B$)

work.[7] η takes a minimum value and becomes close to unity as Re approaches 0, as discussed in the previous work.[7] It can also be seen that η of the Ca^{2+}–H^+ system is larger than that of the K^+–H^+ system. This is because, for the Ca^{2+}–H^+ system, the diffusion coefficient of Ca^{2+} in the membrane is relatively small, as shown in Table 1; hence the mass transfer resistance in the membrane phase becomes relatively larger.

The reasons for the change in $\mathscr{M}_i$ as shown in Fig. 3 can be explained as follows. First, the reason $\mathscr{M}_i$ of the Ca^{2+}–H^+ system is smaller than that of the K^+–H^+ system is that Ca^{2+} has a smaller diffusion coefficient in the membrane. Secondly, the reason $\mathscr{M}_i$ of the Ca^{2+}–H^+ system increases slightly with Re is that this system has larger mass transfer resistance in the membrane.

In industrial separation processes, spacers or nets are often used in the channels to reduce the mass transfer resistance in the liquid phase.[4,8] The spacers promote mixing in the direction normal to the liquid flow. It is desirable to develop a spacer attaining perfect mixing along the y axis with a lower pressure drop. If such an ideal spacer were available and used, the mean dialytic rate would rise to $1/\eta$ times the rate without the spacer. Therefore, the mean dialytic rate of the dialyzer with an actual nonideal spacer can take some value from that calculated by our model (Figs. 3 and 4) to $1/\eta$ times the calculated value.

A larger concentration gradient in the membrane is required for higher dialytic rate. It is necessary for this purpose that the concentrations of K^+ (or Ca^{2+}) in the membrane be higher on the channel A side and lower on the channel B side. For the Ca^{2+}–H^+ system, however, only a slight increase in concentration on the channel A side is expected, since the concentration is close to the ion-exchange capacity as shown in Fig. 6. In contrast, the concentration on the channel B side can decrease considerably. Thus, each channel has a different influence on the overall mass transfer resistance. An effectiveness factor for each channel is then introduced as follows:

$$\eta_A(\text{or } \eta_B) = \frac{(\mathscr{M}_i \text{ calculated considering liquid-phase mass transfer resistance in both channels})}{\{\mathscr{M}_i \text{ calculated ignoring liquid-phase mass transfer resistance in channel } A \text{ (or } B)\}} \quad (14)$$

η_A (or η_B) has a value between 0 and 1. It approaches 0 when the contribution of the liquid-phase mass transfer resistance in channel A (or B) to the overall one is larger, and becomes 1 when that contribution vanishes.

The calculated η_A and η_B values are shown in **Fig. 9**. For the K^+–H^+ system, the η_A and η_B values are close to each other, so the contributions of both channels are considered to be comparable. For the Ca^{2+}–H^+ system, however, η_A is much larger than η_B; that is, the contribution of channel A is much smaller than that of channel B. This is also because bivalent Ca^{2+} is favorably taken into the membrane as against univalent H^+.

Conclusion

Ionic transport in the continuous Donnan dialyzer with two parallel-plate channels was satisfactorily modeled using the mass transfer equations. Simultaneously, a dialytic experiment was carried out for the K^+–H^+ and Ca^{2+}–H^+ exchange systems. The theory was verified by comparison with the experimental results for the mean dialytic rate. The theoretical calculation also provided the distributions of the ionic concentrations and of the electric potential. The influences of Re number, channel height and valence of the counter-ion on the mean dialytic rate and the effectiveness factors were quantitatively elucidated.

Nomenclature

A_{eff}	=	effective area of membrane	[m^2]
C	=	ionic concentration	[$mol \cdot m^{-3}$]
D	=	ionic diffusion coefficient	[$m^2 \cdot s^{-1}$]
F	=	Faraday's constant	[$C \cdot mol^{-1}$]
$K_2{}^1$	=	selectivity coefficient	[—]
L	=	length of dialytic section in the x direction	[m]
$\mathscr{M}_i$	=	mean dialytic rate of ion i	[$equiv \cdot m^{-2} \cdot s^{-1}$]
N_i	=	ionic flux in the direction of the y axis	[$mol \cdot m^{-2} \cdot s^{-1}$]
$\mathscr{N}_{A,i}$	=	dimensionless ionic flux, $N_i/6\bar{u}_A Q$	[—]
$\mathscr{N}_{B,i}$	=	dimensionless ionic flux, $-N_i/6\bar{u}_B Q$	[—]
n_i	=	valence	[—]
Q	=	concentration of fixed ion (ion exchange capacity)	[$mol \cdot m^{-3}$]
R	=	gas constant	[$J \cdot mol^{-1} \cdot K^{-1}$]
Re_h	=	Reynolds number for channel h, $\delta_h \bar{u}_h / v$	[—]
$S_{h,i}$	=	dimensionless ionic diffusion coefficient, $D_i/6\bar{u}_h\delta_h$	[—]
T	=	temperature	[K]
U_h	=	dimensionless velocity, $u_h/6\bar{u}_h$	[—]
u_h	=	velocity in channel h	[$m \cdot s^{-1}$]
$\bar{u}_h$	=	average velocity in channel h	[$m \cdot s^{-1}$]
W	=	width of channel	[m]
X	=	dimensionless x coordinate, x/δ_A	[—]
x	=	coordinate parallel to flow	[m]
Y_A	=	dimensionless y coordinate of channel A, y/δ_A	[—]
Y_B	=	dimensionless y coordinate of channel B, $-(y+\delta_M)/\delta_B$	[—]
y	=	coordinate normal to flow	[m]
Z	=	dimensionless ionic concentration, C/Q	[—]
δ_h	=	height of channel h	[m]
δ_M	=	thickness of membrane	[m]
η	=	effectiveness factor	[—]
η_h	=	effectiveness factor for channel h	[—]
v	=	kinematic viscosity	[$m^2 \cdot s^{-1}$]
Φ	=	dimensionless electric potential, $F\phi/RT$	[—]
Φ_0	=	arbitrary constant	[—]
ϕ	=	electric potential	[V]

〈Subscripts〉

F	=	fixed ion in membrane
h	=	parallel-plate channel ($=A$ or B)
i	=	ionic species (1 : K^+ or Ca^{2+}, 2 : H^+, 3 : Cl^-)
in	=	inlet of channel
out	=	outlet of channel

〈Superscripts〉

—	=	intramembrane phase

Literature Cited

1) Helfferich, F.: "Ion Exchange", p. 153, McGraw-Hill, New York (1962).
2) Helfferich, F.: "Ion Exchange", p. 156, McGraw-Hill, New York (1962).
3) Helfferich, F.: "Ion Exchange", p. 268, McGraw-Hill, New York (1962).
4) Kuroda, O., H. Matsuzaki and S. Takahashi: *Kagaku Kogaku Ronbunshu*, **8**, 240 (1982).
5) Robinson, R. A. and R. H. Stokes: "Electrolyte Solutions", 2nd ed., p. 317, Butterworths Pub., London (1959).
6) Sato, K., T. Yonemoto and T. Tadaki: *J. Membrane Sci.*, **53**, 215 (1990).
7) Sato, K., C. Fukuhara, T. Yonemoto and T. Takaki: *J. Chem. Eng. Japan*, **24**, 81 (1991).
8) Sudoh, M., H. Kamei and S. Nakamura: *J. Chem. Eng. Japan*, **20**, 34 (1987).